Metallurgical and mechanical properties of Al-Cu joint by friction stir spot welding and modified friction stir clinching

Pingqiang Gao[1], Yan Zhang[1,#], Kush P. Mehta[2,3,*]

[1] School of Chemistry and Chemical Engineering, Yulin University, Yulin City, Shaanxi 719000, People's Republic of China
[2] Advanced Manufacturing and Materials research group, Department of Mechanical Engineering, School of Engineering, Aalto University, Espoo, Finland
[3] Department of Mechanical Engineering, School of Technology, Pandit Deendayal Petroleum University, Gandhinagar, Gujarat, India

[*] Corresponding author e-mail: kush_2312@yahoo.com

[#] Co-Corresponding author email: gpqzy203@126.com

Abstract

Dissimilar joints of AA5083 and pure Cu joint are successfully produced and compared by friction stir spot welding and modified friction stir clinching with intermediate layer of Zn interlayer for the first time. Self-reacting behavior of Zn is observed to obtain sound welds resulted from intermixing in stir zone (in FSSW), refilled zone (in MFSC) and brazed zone (in both FSSW and MFSC). MFSC is used to fill the cavity of keyhole that in turn increased 40 % strength of dissimilar Cu-Al joints. Presence of lamellar eutectics in brazed zone and intermetallic compounds such as Al_2Cu, Al_4Cu_9, $CuZn_5$ and Cu_4Zn in weld zone are confirmed in Cu-Al MFSC joints.

Keywords: Al-Cu, dissimilar welding, friction stir spot welding, modified friction stir clinching, microstructural evolution, Zn interlayer

1. Introduction

Dissimilar welding of copper (Cu) and aluminum (Al) materials is greatly useful in the electrical and electronics industries considering excellent properties of electrical and thermal conductivities [1]. However, the sound welding of these two materials is difficult to obtain by fusion welding processes due to defects formation caused by intermetallic compounds (IMCs) and low melting eutectics [2, 3]. Solid state welding is considered as favorable processing condition for Al-Cu joints, as it operates below the melting point and with plastic deformation of materials [4–6]. Being a solid state welding family, friction stir welding (FSW), friction stir spot welding (FSSW), and other friction based welding processes are reported with large numbers in recent literature for different dissimilar combinations including Al-Cu [7–10]. Application of Al-Cu joints such as bus bar (having small width) is popular in different electrical application [11] and aerospace applications [12], wherein spot configuration of welding process is suitable. In study of Heideman et al. [13], FSSW is employed to obtain dissimilar weld of Al-Cu and concluded successful weld formation with micro-interlocking and Cu ring extrusion upward towards Al material while no continues IMCs. Mubiayi et al. [14] performed Al-Cu FSSW and found that the Cu is detached in the form of particles and mixed in Al matrix with formation of IMCs. Shiraly et al. [15] carried out FSSW of Al-Cu with resulted composite type joint of crushed Al-Cu materials and IMCs in the stir zone. Boucherit et al. [16] introduced Zn interlayer between Al-Cu FSSW to improve the mechanical behavior of joints, wherein Cu is kept on Al. In case of FSSW, the formation of exithole/keyhole is a biggest problem, wherein the volumetric material is missing. This keyhole is inevitable due to penetration of tool's probe in workpiece, which is subsequently a location for stress concentration and corrosion initiation [17, 18]. This keyhole can be greatly eliminated using modified friction stir clinching (MFSC) process, wherein protuberance leveling and keyhole filling are obtained in the second phase of process using probeless tool. However, with MFSC, limited articles are published so far, that are on Al base materials. MFSC is investigated on AA2024-AA7075 [19, 20] and AA2024-AA6061 [21] joint combinations. These studies mention that MFSC is emerging as great alternative of FSSW for spot configuration welds. Although, MFSC is never attempted for any dissimilar combination such as Al-Cu. Hitherto, there is no comparison available on Al-Cu welding obtained by FSSW and MFSC. The application of Zn interlayer in Al-Cu spot welding is also limited with metallurgical bonding details. Therefore, it is worthwhile to present an investigation with microscopic evaluation of Al-Cu welds made by FSSW and MFSC. In the present study, the dissimilar welds of Al-Cu are produced by FSSW and MFSC using thin self-reactive Zn interlayer with novel materials mixing comparison and robust metallographic measurements.

2. Materials and methods

In the present investigation, aluminium alloy AA5083 and commercially pure copper consists of thickness 1.5 mm and 2 mm respectively are welded by FSSW and MFSC techniques. The chemical compositions of respective base materials are presented in Table. 1 and Table. 2.

Table. 1 Chemical composition of 5083-H321 aluminum alloy (wt%)

Alloy	**Al**	**Mg**	**Mn**	**Fe**	**Cr**	**Si**
AA5083	Base	4.31	0.63	0.23	0.12	0.11

Table. 2 Chemical composition of pure Cu (wt%)

Alloy	**Al**	**Fe**	**Pb**	**Zn**
Pure Cu	0.0033	0.00061	0.0022	<0.00012

An overlap joint configuration with Cu on top of Al base material is selected with a self-reacting layer of Zn (with 99.99 wt.% purity and 100 µm thickness) kept intermediate between both base materials [see Fig. 1 (a)]. FSSW and MFSC processes are performed with constant parameters such as 1200 rpm of rotational speed, 6 seconds of dwell time and 0.4 mm of shoulder penetration depth. H13 tool material is used for the experimentation of FSSW and

MFSC. FSSW is performed using tool consists of 10 mm shoulder diameter (with 6° concave surface) and concave probe of 4 mm root diameter 2.5 mm tip diameter and 2.6 mm probe length. MFSC's first step is performed using this same tool design used in FSSW using die below the workpiece, and second step is performed by probe-less tool of 14 mm shoulder diameter. The repeatability of processing conditions is confirmed by number of weld formation at least three times for each condition. After the welding, the specimens are subjected to optical and scanning electron microscopies (SEM), energy dispersive x-ray spectroscopy (EDX), X-ray diffraction (XRD) analysis, electron back scattered diffractions (EBSD) analysis and tensile/shear testing to evaluate the joint properties differences. Standard metallographic procedure (of grinding, polishing and chemical etching) is performed with chemical etching by the solution of H_2O 50 cc, HCl 10 cc and 2 grams $FeCl_3$. for metallurgical characterization. Computerized universal testing machine (INSTRON 5500R) is used to perform tensile/shear test as per standard dimension shown in Fig. 1 (b), at a crosshead speed of 1 mm/min.

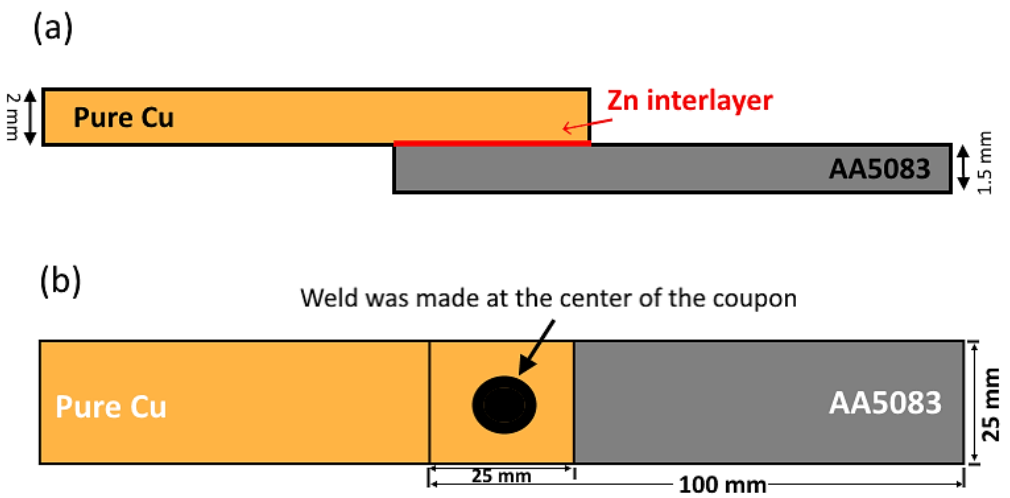

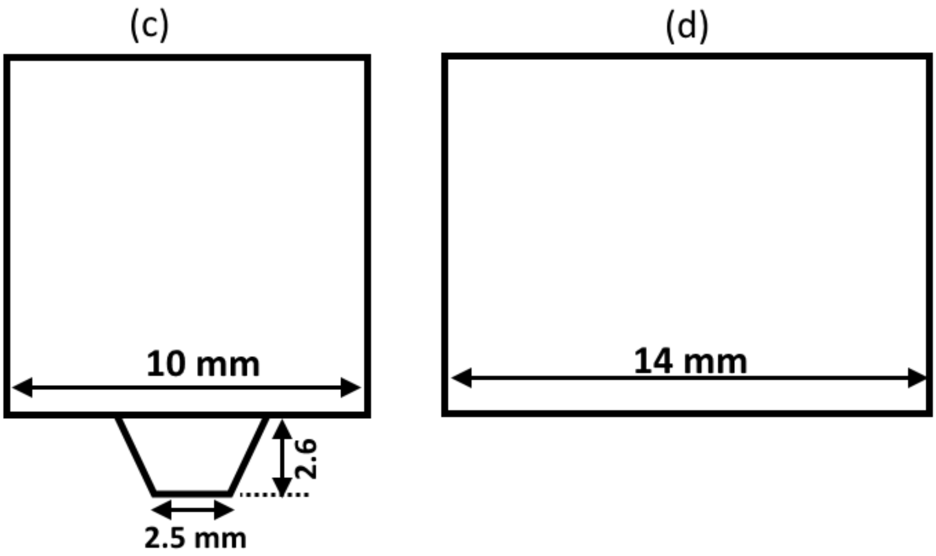

Fig. 1 (a) Cu-Al overlap configuration with Zn interlayer; (b) tensile/shear sample, (c) dimensions of tool used for FSSW and first phase of MFSC and (d) dimensions of tool used in second phase of MFSC

3. Results and discussion:

Cu-Al joint by FSSW with Zn interlayer is shown in Fig. 2 with its cross-sectional macro view, microstructures, and SEM-EDX. The keyhole is clearly observed at the probe location while shoulder insertion depth as can be seen from Fig. 2 (a). However, no discontinuities are observed in the material mixing regions that are at the surrounding of keyhole's indentation. The stirring action is caused by probe where the mixing of materials can be observed from Fig. 2 (b) and (c) while the interface region under the shoulder and outside of stirring zone can be observed with Cu-Zn-Al brazed zone [see Fig. 2 (a)]. This brazed zone is observed with dendritic pattern of Zn alloying layer consists of Cu material penetration into it. This is caused due to subjected heat under shoulder surface with self-reacting phenomenon of Zn accompanied by localized melting and diffusion of Cu and Al materials. The diffusion participation of Cu-Zn-Al materials is evidenced by EDX analysis such as 15.31 % weight of Al, 32.79 % weight of Cu and 51.91 % weight of Zn at dendritic location as can be seen from Fig. 2 (a). The dendrite like shape at the transition region near the Cu-side is likely consists of IMCs of Cu_4Zn and $CuZn_5$ based on ternary diagram of Al-Zn-Cu that shows a coherent matching between the chemical compositions of the transition region and the Cu-phase. The presence of these IMCs can also be correlated with diffusive temperature occurred in FSSW process that is generally 80% of the melting temperature (i.e. around 400°C at the interface of tool and workpiece). In case of Fig. 2 (a) this conducted temperature kept Cu-Zn-Al in solid state and resulted in formation of IMCs in dendritic like shapes. Zn material is chemically compatible with Al and Cu base materials to experience self-propagating reaction. Similar type of self-reacting phenomenon of Zn with Cu and Al is observed in the published work of [22]. Besides, the stirring action caused by probe of tool is responsible for materials strain effects with plastic deformation. This plastic deformation is subsequently responsible for joint formation after recrystallization. Since the deformation behavior between Cu and Al is different at subjected heating condition, the complex stir zone is observed in Fig. 2 (b) and Fig. 2 (c). It can be seen that this stir zone is a location where materials mixing is successfully established. However, differences in stir zone region is caused with no specific accumulation of single-phase regions, representative of any phase segregation. This mixing is observed as complex in terms of different fragments of Cu randomly mixing in Al matrix due to strong stirring action, which is subsequently confirmed by elemental mapping as shown in Fig. 2 (d). However, the presence of Zn is also found in large percentage that is obvious. Therefore, it can be said from Fig. 2 (d) that the EDX elemental mapping shows that the atomic ratio of Al:Cu: Zn is about 2:2:1 that indicates the formation of complex compositions/phases such as (Al_2Cu+Al_4Cu_9+$CuZn_5$+Cu_4Zn) at this specific region. This stir region consists of different local variations in microstructures can be treated as composite structure. Aforementioned brazed layer may also present inside the stir zone in micro and nano level that in turn establishes the metallurgical bonding of Al and Cu with Zn presence and hence that can prevent the formation of the major discontinuities.

Stir zone of Fig. 2 (b) region is generated at the time of retraction phase of probe wherein the Al material is also participated due to movements of stirring and retraction. Besides, stir zone of Fig. 2 (c) is generated beneath the probe surface at the time of plunge phase that can be indicated as the shearing bending patterns beneath the probe profile. The penetration of Cu material in Al material can also be referred as mechanical hooking effect. This specific feature beneath the keyhole is similar to squeezed flow patterns created by the extrusion forces induced by probe of the tool. Higher deformation of Cu material at the corner of probe's surface can be evidenced from Fig. 2 (c). However, no Cu ring formation occurred such as reported in literature of [13, 14] that is considered as non-favorable features. The participation of Al-Zn-Cu materials can also be seen from Fig. 2 (c)'s higher magnification image, wherein lamellar eutectics are observed with metal matrix type composites structure with Al matrix and Cu fragments. The bonding between Al-Cu with Zn intermediate material is expected with formation of IMCs in this zone too. In the stir zone region at Al side (matrix region in Fig. 2 (b) and (c)), the grain refinement can be observed that resulted in ultrafine equiaxed grain structure. The EDX elemental mapping of Fig. 2 (d) and (c) show uniformly distribution of elements of Al, Cu and Zn within the stir zone region that subsequently indicates uniform elemental interaction between each other. However, these interactions under subjected heating and loading conditions form IMCs and eutectic phases with these interactions, which is confirmed later with XRD analysis.

(a)

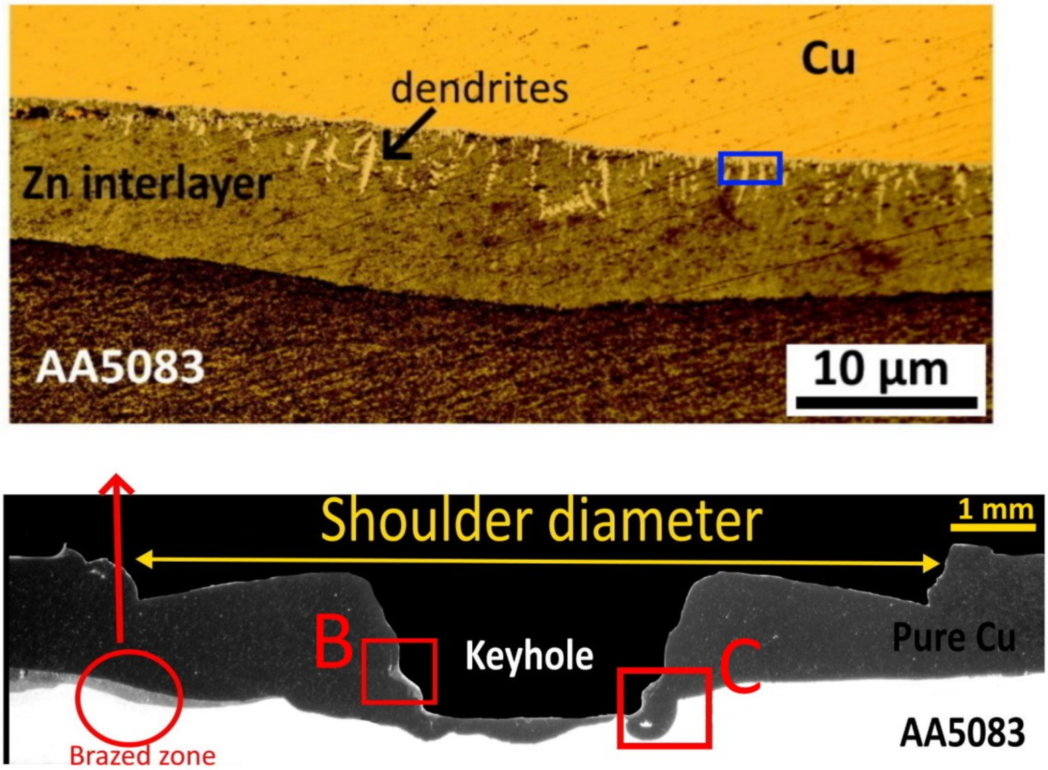

Cu
dendrites
Zn interlayer
AA5083
10 µm
Shoulder diameter
1 mm
B
Keyhole
C
Pure Cu
Brazed zone
AA5083

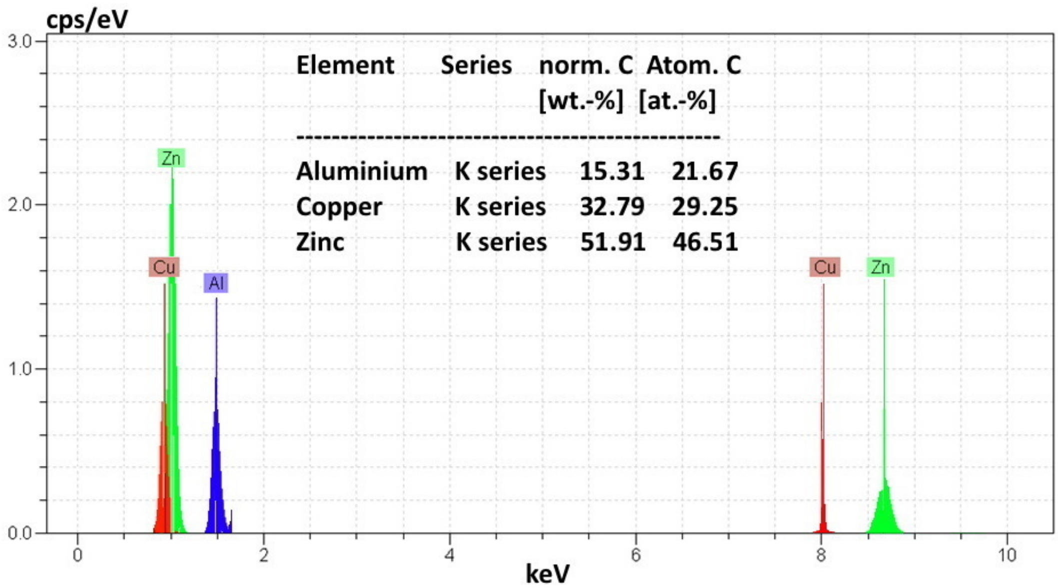

cps/eV
Element Series norm. C [wt.-%] Atom. C [at.-%]
Aluminium K series 15.31 21.67
Copper K series 32.79 29.25
Zinc K series 51.91 46.51
Zn
Cu
Al
Cu
Zn
keV

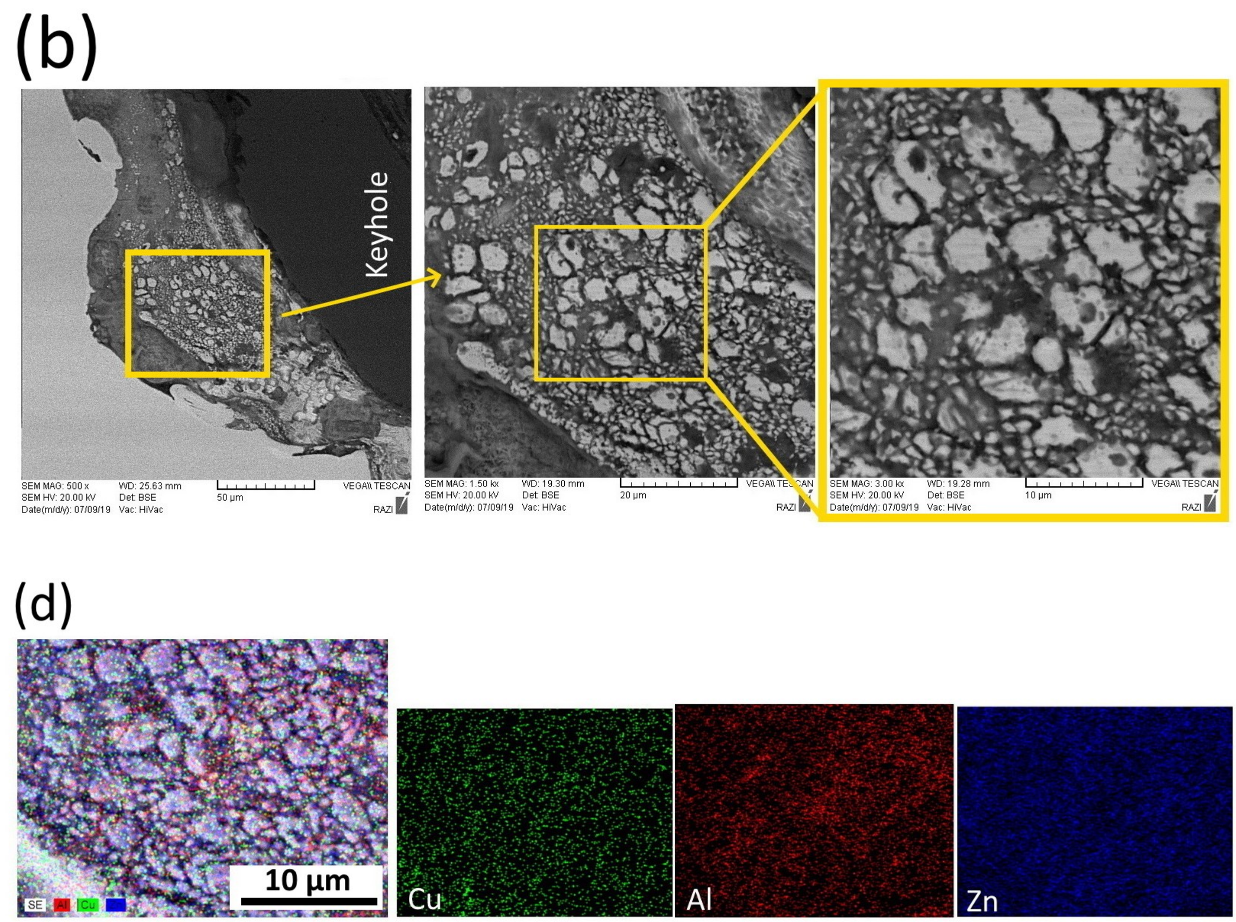

Fig. 2 FSSW Cu-Al weld interface, (a) optical macrostructure and Al-Zn-Cu interface outside of stir zone, (b) SEM images stir zone, (c) SEM images of stir zone and IMCs and (d) elemental mapping of Image 2b.

Cu-Al joint by MFSC with Zn interlayer is shown in Fig. 3 with its cross-sectional macro view, microstructures, and SEM-EDX images. It can be seen from Fig. 3 (a) that the keyhole is greatly filled when probe-less tool is subjected from the revert side of the clinched zone with 0.4 mm indentation of shoulder on workpiece of Al. The complex mixing can be evidenced from Fig. 3 (a), wherein the materials experienced deformation two times with two different phases such as (1) the stirring during first phase and (2) the forging during second phase. During stirring action, the Cu is contacted by shoulder while probe is stirred and plunged up to Al material through Zn interlayer that in turn extract the material downward in the die, whereas the extracted material during first phase is forged towards keyhole cavity by reverting the workpiece, wherein the shoulder is subjected to Al material that in turn make indentation of shoulder's diameter. The refilling is caused due to intermixing between Al-Zn-Cu materials with layered structures. These layers are of different size that are caused due to plastic deformation by forging action at the time of second phase. Large bulk of each Al-Zn-Cu materials is deformed that in turn resulted with lumped layers consists of those bulk materials. Besides, no such lumped layers of Al-Zn-Cu are observed in case of FSSW as no refilling phase is performed. The micro images of Fig. 3 (a) shows interpenetration of bulk material with mechanical interlocking phenomenon in the center region where keyhole filling is performed. Similar type of material occurred in case of keyhole repairing of Al-Mg FSW [18]. The interface of bulk AA5083 and Cu in the same zone is observed with heterogeneous grain refinements and formed a diffusive layer [refer SEM image of Fig. 3 (a)]. The presence of IMCs and eutectics is expected in this region. Therefore, SEM with spot EDX are performed as can be seen from Fig. 3 (a). From the elemental results [refer EDX (spot of A, B, C, D) and SEM image of Fig. 3 (a)], it can be indicated that different phases and compositions are presented at this interface. Presence of IMCs can be predicted from EDX elemental analysis of point A, B and D. Point A is observed with 45.21 % weight of Al and 53.95 % weight of Cu that can be predicted as IMC of $CuAl/CuAl_2$. This phase is distributed in heterogenous way as can be seen from SEM image of Fig. 3 (a). Point B indicates similar composition of Al and Cu that shows distribution of similar IMC phase of $CuAl/CuAl_2$ within shown region of Al-Cu interface. Point C shows elements of 93.87 % weight of Al and 6.13 % weight of Cu that indicate Al rich solid solution in the form of matrix/solvent with small Cu solute. In case of point D, 68.60 % weight of Zn, 24.47 % weight of Cu and 6.93 % weight of Al is observed in EDX image that subsequently indicates formation of Zn rich IMC of $CuZn_5$. However, the exact phase formation is identified by XRD analysis that is presented later in subsequent section. Solid state diffusion is driving phenomenon for the formation of these IMCs and other phases [23]. In case of FSSW of Al-Cu, the formation of IMCs are restricted to a small zone of stirring action while in case of MFSC, the formation of IMCs can also be expected in the filled keyhole zone. On the other hand, outside of refilled zone, the Zn interlayer is brazed with Al and Cu similar to observed with FSSW. However, the formation of lamellar eutectics and anomalous eutectic are clearly observed in large amount in this zone that in turn confirms brazing of Zn with individual interactions of Al and Cu. This lamellar morphology of grain structure also attributed to the mixed chemical composition of the eutectic region due to an interaction between Al-Zn-Cu, which is resulting in the formation of a new eutectic phase at the interface bonding layer of dissimilar Al-Cu weld [22]. The self-reaction of Zn is occurred within conducted heat from shoulder interaction at the time of friction stir clinching as well as refilling phases. Compare to FFSW Al-Cu brazed zone, the brazed zone of MFSC Al-Cu is found more uniform. In Fig. 2 (b), the indented cavity towards Cu side is found with Zn rich solid solution such as (point E: 73.39 % weight of Zn, 15.15 % weight of Cu and 5.30 % weight of Al) and (point F: 68.18 % weight of Zn, 13.99 % weight of Cu and 17.83 % weight of Al). This is occurred at the time of first phase wherein stick material on tool (i.e. used tool with Al-Zn-Cu combination) is deposited in-side the cavity when the first phase of MFSC is performed.

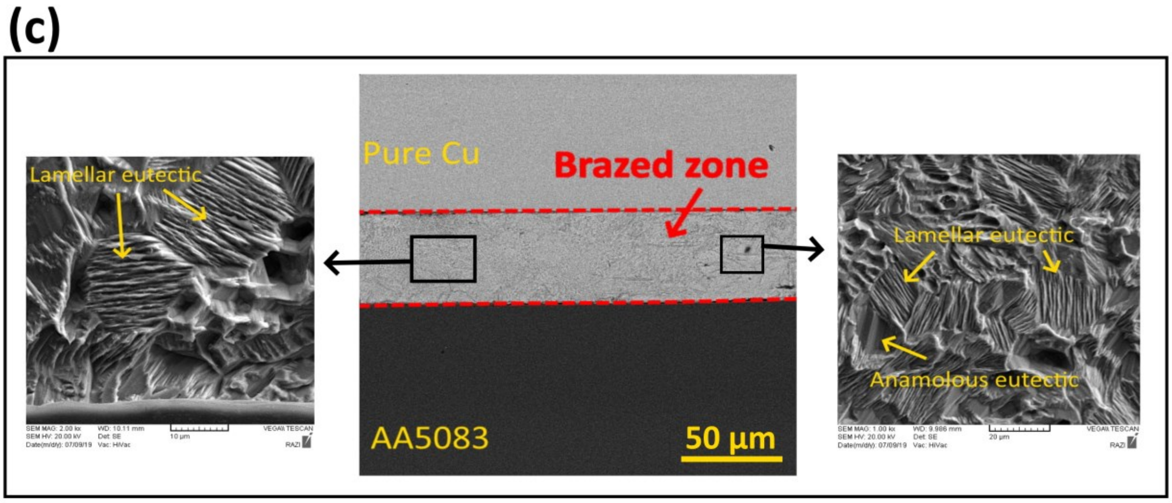
(c)
Pure Cu
Brazed zone
Lamellar eutectic
Lamellar eutectic
Anamolous eutectic
AA5083
50 µm

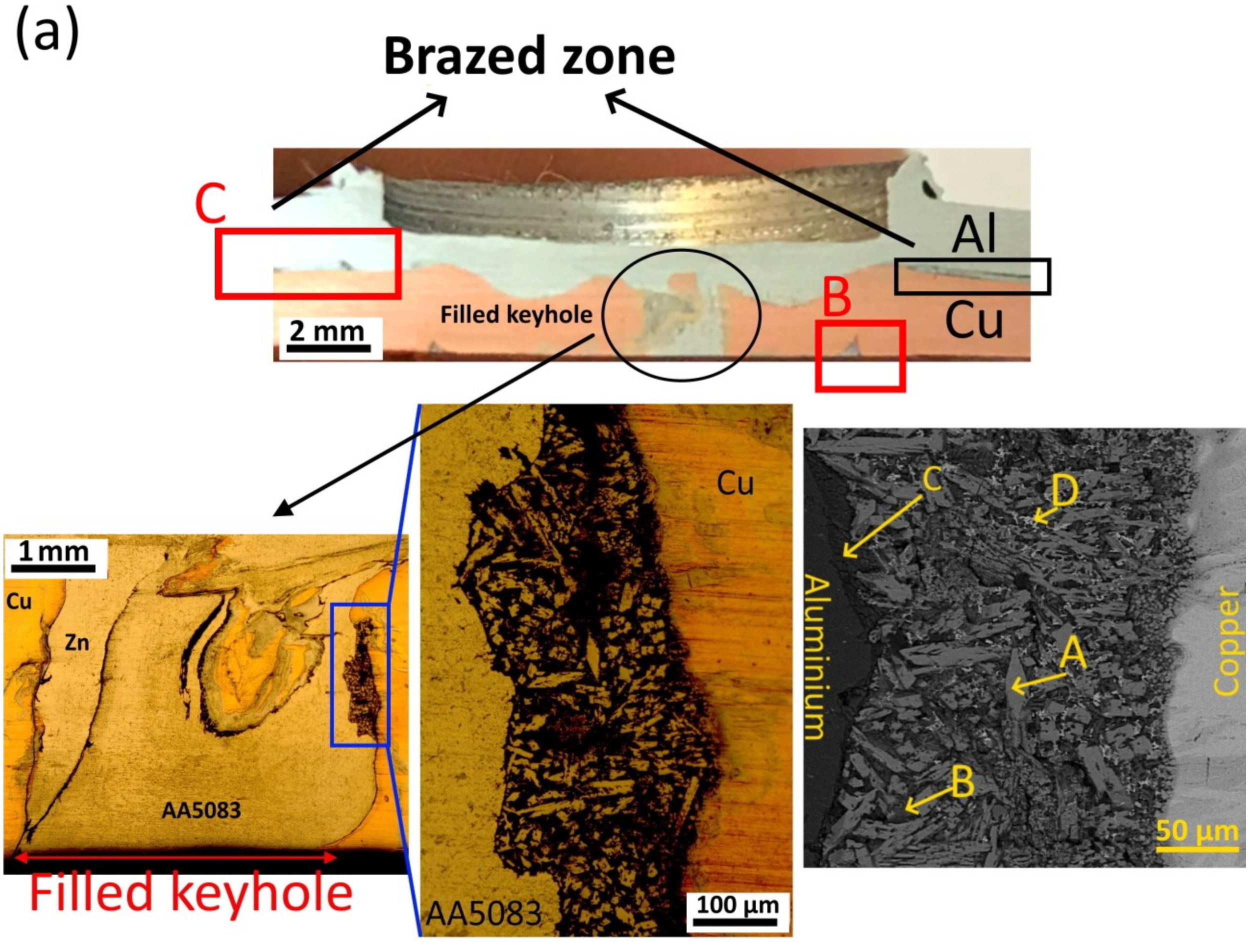
(a)
Brazed zone
C
Al
B
Cu
Filled keyhole
2 mm
1 mm
Cu
Zn
AA5083
Filled keyhole
Cu
AA5083
100 µm
C
D
Aluminium
A
Copper
B
50 µm

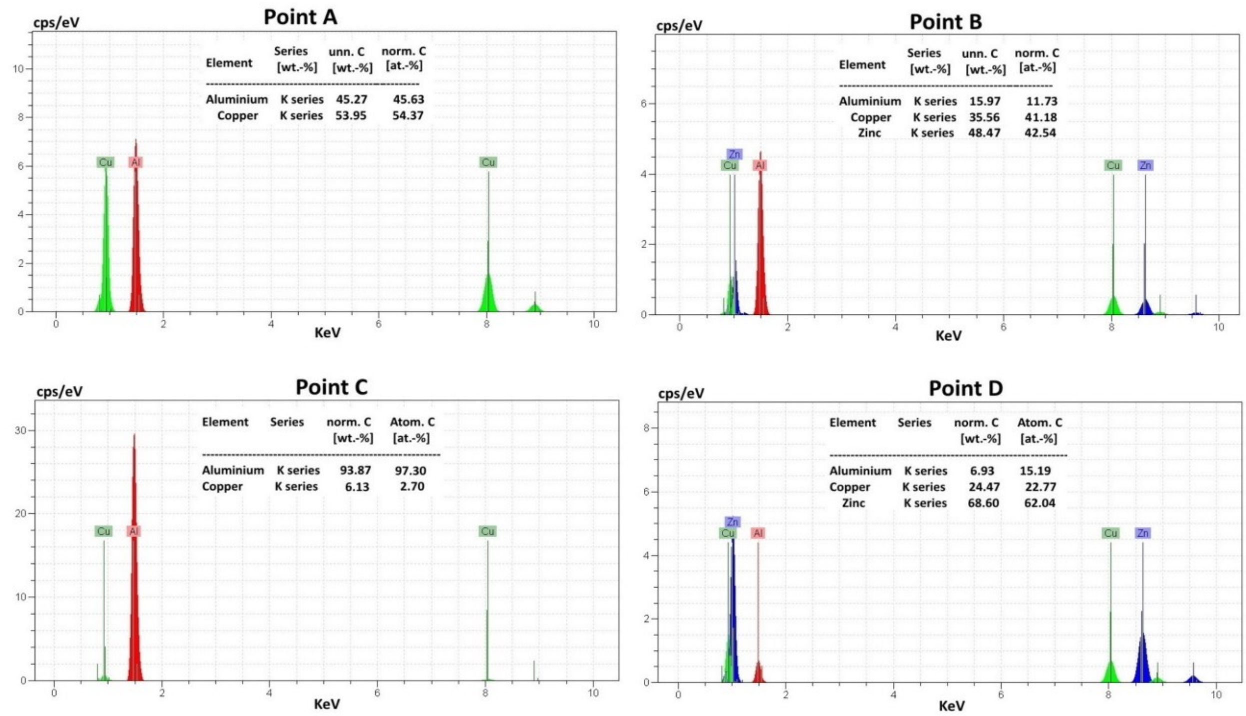

(b)

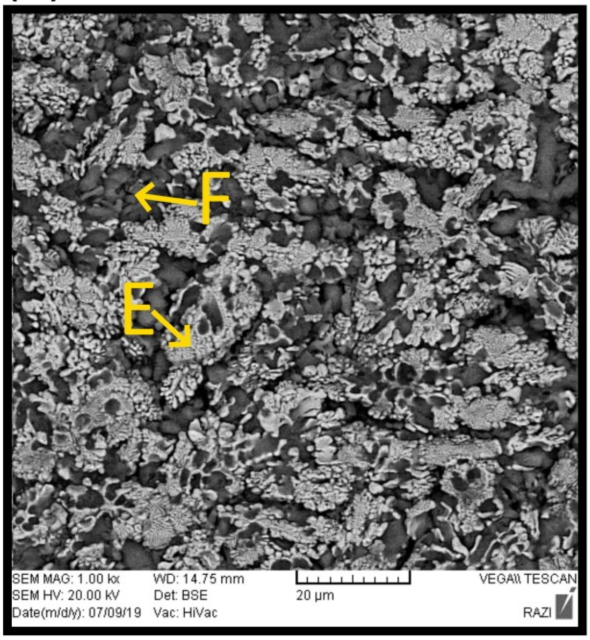

Point E

Element	Series	unn. C [wt.-%]	norm. C [wt.-%]	Atom. C [at.-%]
Aluminium	K series	5.30	4.77	6.87
Copper	K series	15.15	14.51	17.19
Zinc	K series	73.39	80.71	75.94

Point F

Element	Series	unn. C [wt.-%]	norm. C [wt.-%]	Atom. C [at.-%]
Aluminium	K series	17.83	13.68	29.27
Copper	K series	13.99	15.72	14.21
Zinc	K series	68.18	70.60	56.52

Fig. 3. MFSC Al-Cu weld interface, (a) Optical macrostructure, keyhole filled zone and spot EDX results, (b) SEM images from brazed zone, (c) SEM images and elemental distribution underneath of filled keyhole.

Fig. 4 shows microstructural differences of stir zone towards Cu side for FSSW and MFSC welds represented by (a)-(d) and (e)-(h) respectively. It can be seen that no major variations in grains of FSSW are observed Fig. 4 (a), whereas variations in grain size is observed for MFSC condition [see Fig. 4 (e)]. These differences are in line with aforementioned differences in processing conditions where intense and severe deformation is occurred in stir zone of FSSW that subsequently resulted with equiaxed uniform grains. Besides, second phase of MFSC is performed wherein crushing of material is carried out with large bulk of base material without stirring effect that subsequently resulted with differences in grain size. Inverse pole figure (IPF) comparison between Fig. 4 (b) and Fig. 4 (f) show that crystal orientations are also random due to complex processing between dissimilar materials of Al and Cu with Zn interlayer. In case of FSSW, the grains of IPF maps are majorly in between [111] and [001] with few grains in [101], whereas the grains of IPF maps in case of MFSC are more in between [101] to [111] with presence of few grains in [001]. In both of the processing conditions, [001] grains and other grains composed of [101] and near [101] are showing twinning behavior that is typically observed in Cu material. Low angle grain boundaries of 1065 with 0.80 mm length in between 2° to 5° are observed, whereas the grain boundaries of 321 with 123.04 microns in between 5° to 15° are observed in case of FSSW. High angle grain boundaries of 15682 with 1.04 cm length in between 15° to 180°are observed [refer Fig. 4 (c)-(d), (g)-(h)]. Additionally, some amount of grain misorientation can also be observed in case of MFSC compared to the FSSW sample due to strong stirring action.

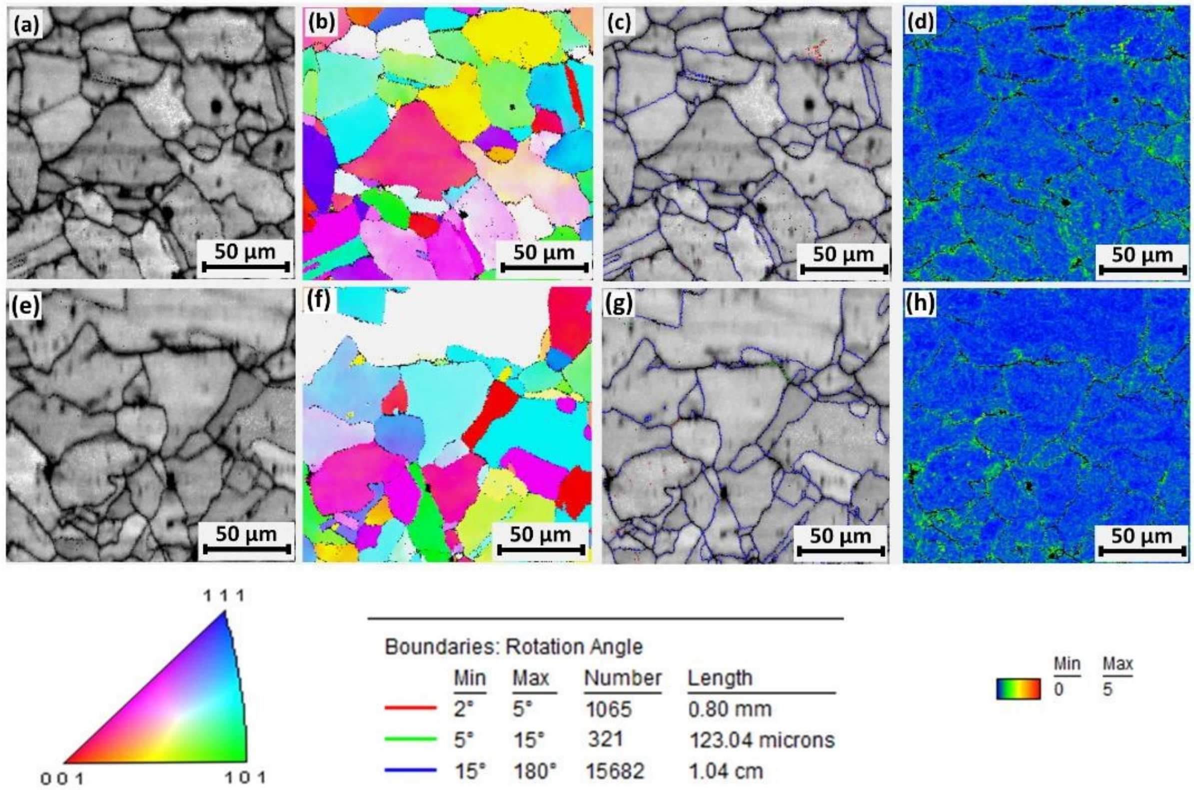

Fig. 4 Microstructural differences in stir zone toward Cu side (a)-(d) FSSW and (e)-(h) MFSC.

Fig. 5 shows details on failure load of tensile testing, fracture surface analysis by SEM image and XRD analysis for phase identification. Despite of bulk material evidence in weld zone (i.e. keyhole filled zone) in case of MFSC, higher tensile-shear failure load of 7369 N is observed [see Fig. 5 (a)]. The failure load of tensile-shear testing is 4597 N in case of FSSW even after intense stirring-mixing process [see Fig. 5 (a)]. The tensile strength is increased by about 40% for the MFSC, as compared to the FSSW. This is attributed to keyhole effect that is a big major difference between FSSW and MFSC. During tensile testing, the specimens are fractured from keyhole surface as the volumetric material is missing and stresses are concentrated at the point of keyhole's surface. Besides, the MFSC tensile specimens are fractured from interface (refilled zone) region. The fractured surface of tensile specimen from the weld of MFSC sample is shown in Fig. 5 (b), wherein the features of large flat surfaces and dimples are evidenced. In general, Al and Cu alloys show ductile fracture mode because of its maximum slip systems of face centered cubic (FCC) structure. In FCC metal, flat and smooth fracture surface can be possible after tensile testing where its ductility is consumed by severe plastic deformation. However, in this case of Al-Cu joining, dominant brittle fracture with local ductile fractures modes can be predicted due to formation of IMCs. The brittle fracture mode is caused due to IMCs formation at the interface region as predicted in previous discussion. These IMCs are hard and brittle in nature that are prone to create cracks in loading conditions [1, 5, 23]. Therefore, the tensile specimens are fractured with brittle fracture mode indications. The formation of IMCs is confirmed by XRD analysis as shown in Fig. 5 (c). From the XRD analysis, it can be seen that the welding zone is complex mixture of different phase and compositions, wherein binary phase of Al-Cu materials such as Al_2Cu and Al_4Cu_9 along with binary phase of Cu-Zn such as $CuZn_5$ and Cu_4Zn are observed. An obvious presence of Al and Zn single phases are also reported. These phases are in line with above discussions supported by SEM-EDX analysis and are also matching with published literature of [16, 22]. This subsequently also proves local intermixing and solid-state diffusion with favorable processing conditions required to obtain bonding between dissimilar materials.

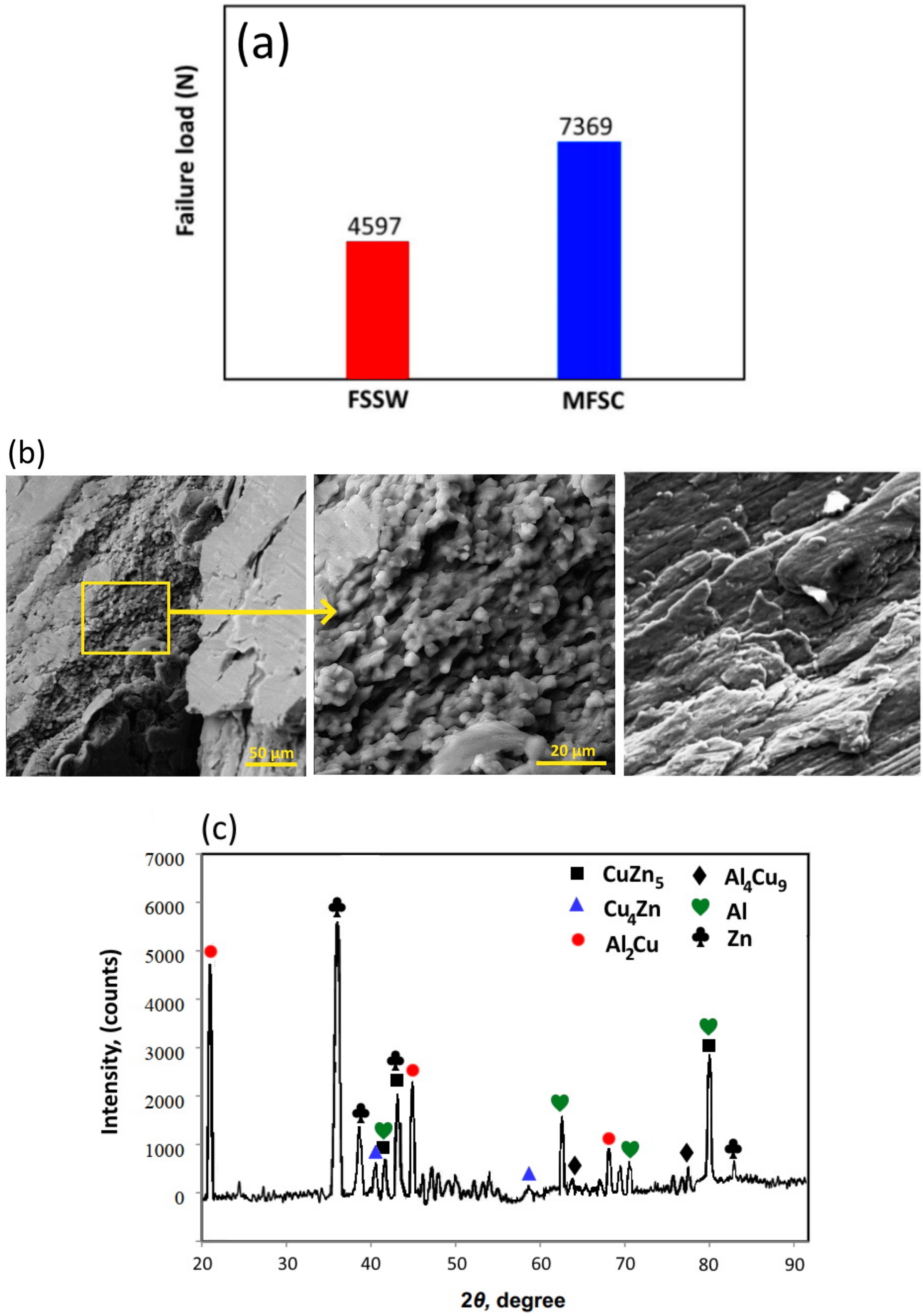

Fig. 5 (a) Failure load details of FSSW and MFSC of Al-Cu joints, (b) fractured surfaces and (c) XRD analysis of MFSC.

4. Conclusions

Friction stir spot welding (FSSW) and modified friction stir clinching (MFSC) are successfully performed to obtain sound dissimilar Cu-Al joints using Zn interlayer material. Self-reacting behavior of Zn with Al-Cu combination in solid state processing is observed to obtain sound welds resulted from intermixing in stir zone (in FSSW), refilled zone (in MFSC) and brazed zone (in both FSSW and MFSC). MFSC is used to fill the cavity of keyhole with Al-Zn-Cu bulk material participation that in turn increased 40 % strength of dissimilar Cu-Al joints. Presence of lamellar eutectics in brazed zone and intermetallic compounds such as Al_2Cu, Al_4Cu_9, $CuZn_5$ and Cu_4Zn in weld zone are confirmed in Cu-Al MFSC joints.

Acknowledgements

Innovative Talents Promotion Planning Project of the Science and Technology Department of Shaan Xi (2018KJXX-078); Science and Technology Planning Project of State Administration for Market Regulation (2019MK069); Science and technology of Chongqing science committee Yulin in 2019.

References

1. Mehta KP, Badheka VJ (2016) A review on dissimilar friction stir welding of copper to aluminum: Process, properties, and variants. Mater Manuf Process 31:233–254. https://doi.org/10.1080/10426914.2015.1025971

2. Kah P, Vimalraj C, Martikainen J, Suoranta R (2015) Factors influencing Al-Cu weld properties by intermetallic compound formation. Int J Mech Mater Eng 10:. https://doi.org/10.1186/s40712-015-0037-8

3. Hoseini-Athar MM, Tolaminejad B (2016) Interface morphology and mechanical properties of Al-Cu-Al laminated composites fabricated by explosive welding and subsequent rolling process. Met Mater Int 22:670–680. https://doi.org/10.1007/s12540-016-5687-4

4. Mehta K (2017) Advanced Joining and Welding Techniques: An overview. In: Gupta K (ed) Advanced Manufacturing Technologies. Materials Forming, Machining and Tribology. pp 101–136.

5. Mehta KP, Badheka VJ (2016) Effects of tilt angle on the properties of dissimilar friction stir welding copper to aluminum. Mater Manuf Process 31:255–263. https://doi.org/10.1080/10426914.2014.994754.

6. A. Safarzadeh, M. Paidar, H. Youzbashi-zade (2016) A Study on the Effects Bonding Temperature and Holding Time on Mechanical and Metallurgical Properties of Al–Cu Dissimilar Joining by DFW, Transactions of the Indian Institute of Metals 70, 125–131.

7. Shankar S, Vilaça P, Dash P, et al (2019) Joint strength evaluation of friction stir welded Al-Cu dissimilar alloys. Measurement 146:892–902. https://doi.org/10.1016/j.measurement.2019.07.019

8. Mehta KP (2019) A review on friction-based joining of dissimilar aluminum – steel joints. J Mater Res 34:78–96. https://doi.org/10.1557/jmr.2018.332

9. Mehta KP, Badheka VJ (2017) Influence of tool pin design on properties of dissimilar copper to aluminum friction stir welding. Trans Nonferrous Met Soc China 27:36–54. https://doi.org/10.1016/S1003-6326(17)60005-0

10. Mehta KP, Carlone P, Astarita A, et al (2019) Conventional and cooling assisted friction stir welding of AA6061 and AZ31B alloys. Mater Sci Eng A 759:252–261. https://doi.org/10.1016/j.msea.2019.04.120

11. Ólafsson D, Vilaça P, Vesanko J (2020) Multiphysical characterization of FSW of aluminum electrical busbars with copper ends. Weld World 64:59–71. https://doi.org/10.1007/s40194-019-00814-0.

12. M. Elsa, A. Khorram, O. O. Ojo and M. Paidar (2019) Effect of bonding pressure on microstructure and mechanical properties of aluminium/copper diffusion-bonded joint, Sādhanā 44, 126.

13. Heideman R, Johnson C, Kou S (2010) Metallurgical analysis of Al/Cu friction stir spot welding. Sci Technol Weld Join 15:597–604.

14. MUBIAYI MP, AKINLABI ET (2016) Evolving properties of friction stir spot welds between AA1060 and commercially pure copper C11000. Trans Nonferrous Met Soc China 26:1852–1862.

15. Shiraly M, Shamanian M, Toroghinejad MR, Ahmadi Jazani M (2014) Effect of tool rotation rate on microstructure and mechanical behavior of friction stir spot-welded Al/Cu composite. J Mater Eng Perform 23:413–420.

16. Boucherit A, Avettand-Fènoël MN, Taillard R (2017) Effect of a Zn interlayer on dissimilar FSSW of Al and Cu. Mater Des 124:87–99.

17. Mehta KP, Patel R (2019) On fsw keyhole removal to improve volume defect using pin less tool. Key Eng Mater 821 KEM:215–221.

18. Mehta KP, Patel R, Vyas H, et al (2020) Repairing of exit-hole in dissimilar Al-Mg friction stir welding: Process and microstructural pattern. Manuf Lett 23:67–70.

19. Paidar M, Ojo OO, Moghanian A, et al (2019) Modified friction stir clinching with protuberance-keyhole levelling: A process for production of welds with high strength.

J Manuf Process 41:177–187.

20. Paidar M, Ghavamian S, Ojo OO, et al (2019) Modified friction stir clinching of dissimilar AA2024-T3 to AA7075-T6: Effect of tool rotational speed and penetration depth. J Manuf Process 47:157–171.

21. Paidar M, Vaira Vignesh R, Moharrami A, et al (2020) Development and characterization of dissimilar joint between AA2024-T3 and AA6061-T6 by modified friction stir clinching process. Vacuum 176:109298.

22. Zhang GF, Zhang K, Guo Y, Zhang JX (2014) A Comparative Study of Friction Stir Brazing and Furnace Brazing of Dissimilar Metal Al and Cu Plates. Metallogr Microstruct Anal 3:272–280.

23. Mehta KP, Badheka VJ (2017) Hybrid approaches of assisted heating and cooling for friction stir welding of copper to aluminum joints. J Mater Process Technol 239:336–345.